Frustrated Radical Pairs: From Fleeting Intermediates to Isolable Species

van der Zee, L.J.C.; Hofman, J.; Mathew, S.; de Visser, A.; Bruck, E.; de Bruin, B.; Slootweg, J.C.

DOI
10.1002/chem.202403885

Publication date
2025

Document Version
Final published version

Published in
Chemistry-A European Journal

License
CC BY

Chemistry–A European Journal
Research Article
doi.org/10.1002/chem.202403885
Chemistry Europe
European Chemical Societies Publishing
www.chemeurj.org

Frustrated Radical Pairs: From Fleeting Intermediates to Isolable Species

Lars J. C. van der Zee,[a] Jelle Hofman,[a] Simon Mathew,[a] Anne de Visser,[b] Ekkes Brück,[c] Bas de Bruin,[a] and J. Chris Slootweg*[a]

We present the design and comprehensive investigation of stable *para*-substituted triarylamine–2,3-dichloro-5,6-dicyano-1,4-benzoquinone (DDQ) radical ion pairs (RIPs) generated via single-electron transfer (SET). We quantified the degree of SET in both solution and solid phases, utilising a suite of spectroscopic techniques including IR, EPR, NMR, and single-crystal X-ray diffraction (SC–XRD). Our findings reveal that the extent of SET is significantly influenced by the nature of the substituents (MeO > ^{t}Bu > Br) and the polarity of the solvent (MeCN > DCM > toluene). The radical ion pair $[(p\text{MeOPh})_3\text{N}]^{\bullet+}[\text{DDQ}]^{\bullet-}$ was unambiguously identified using EPR and UV–vis spectroscopy, and its structure was confirmed by SC–XRD. Detailed analysis indicates an open-shell singlet ground state with a thermally accessible triplet state, as corroborated by EPR, magnetic susceptibility measurements, and DFT calculations. This study offers crucial insights into the mechanistic pathways of RIP formation and tuning both in solution and solid states, laying the groundwork for future exploration of their reactivity and potential applications.

Introduction

Organic radical ion pairs (RIPs), comprised of a radical cation and a radical anion, can be formed through single-electron transfer (SET) from a neutral electron donor to a neutral electron acceptor. Typically, radicals are short-lived intermediates in redox reactions,[1] suggesting that pairs of radicals would exhibit even shorter lifetimes due to their propensity for facile back-electron transfer. Consequently, the isolation and full characterisation of stable RIPs in solution and in the solid state has been limited, even though such systems could provide much-needed insights to advance the potential for homolytic bond activation of inert and difficult-to-polarize substrates.

In 1984, Kaim reported the simultaneous observation of both donor and acceptor radical ions by EPR spectroscopy upon mixing the electron-rich *N*-silylated 1,4-dihydropropyrazines **1** with either tetracyanoethylene (TCNE) or tetracyanoquinodimethane (TCNQ),[2] providing the first direct evidence of thermal single-electron transfer involving main group reductants (Scheme 1a). Steric effects played an essential role in enabling the observation of RIPs, as the combination of the bulky bis(triisopropyl)silylated **1** ($E_{ox} = -0.35$ V) and TCNE ($E_{red} = +0.33$ V vs. SCE) in DCM afforded the persistent solvent-separated $[\mathbf{1}]^{\bullet+}[\text{TCNE}]^{\bullet-}$ even at room temperature, but lacked further characterisation beyond EPR evidence. The use of planar electron donors and acceptors is well established in material science for semiconducting applications.[3] However, the use of pnictogen-based donors remains limited. Wang et al. used bis-amine-based electron donors, which, in combination with Lewis acid-activated quinones, afforded the $B(C_6F_5)_3$-coordinated radical ion pairs **2** and **3** through thermal SET (Scheme 1b).[4–6]

Interestingly, even in single electron donor−acceptor systems including the ubiquitous frustrated Lewis pairs (FLPs), recent studies have documented SET events. However, these reports often only reveal single radicals derived from either the Lewis acid or base.[7,8] For the archetypical FLPs $PMes_3/B(C_6F_5)_3$, $PtBu_3/B(C_6F_5)_3$, and analogous N/B systems, we established that visible light induces SET to generate the corresponding transient RIPs $[PR_3]^{\bullet+}[B(C_6F_5)_3]^{\bullet-}$.[9] These photo-generated frustrated RIPs are fleeting intermediates with lifetimes on the order of picoseconds, as determined by transient absorption spectroscopy (i.e., $PMes_3^{\bullet+}/B(C_6F_5)_3^{\bullet-}$ 237 ps; $PtBu_3^{\bullet+}/B(C_6F_5)_3^{\bullet-}$ 6 ps).[8a]

Enhancing the electron affinity of the electron acceptor by complexation with quinones makes the electron transfer thermally feasible[6,8b] and thus substantially increases the concentration of the formed RIPs. Using the bulky phosphine $PTip_3$ (Tip = 2,4,6-*i*Pr$_3$C$_6$H$_2$), we detected both radicals of the RIPs $[PTip_3]^{\bullet+}[\text{quinone–B}(C_6F_5)_3]^{\bullet-}$ **4** at ambient temperatures by UV–vis and X-band EPR spectroscopy (Scheme 1c).[10] However, their inherent reactivity induced homolytic C–H bond activation, precluding full characterization of the RIPs. Furthermore, the use of $PMes_3$ led to quenching of the RIP through the formation of P–O adducts. To induce electronic frustration and prevent such adduct formation,[11] we switched to arylamines as the

[a] L. J. C. van der Zee, J. Hofman, S. Mathew, B. de Bruin, J. Chris Slootweg
Van't Hoff Institute for Molecular Sciences, University of Amsterdam, PO box 94157, 1090 GD Amsterdam, The Netherlands
E-mail: j.c.slootweg@uva.nl

[b] A. de Visser
Van der Waals-Zeeman Institute for Experimental Physics, University of Amsterdam, PO box 99485, 1090 GL Amsterdam, The Netherlands

[c] E. Brück
Fundamental Aspects of Materials and Energy, Department of Radiation Science and Technology, TU Delft, Mekelweg 15, 2629JB Delft, the Netherlands

Supporting information for this article is available on the WWW under https://doi.org/10.1002/chem.202403885

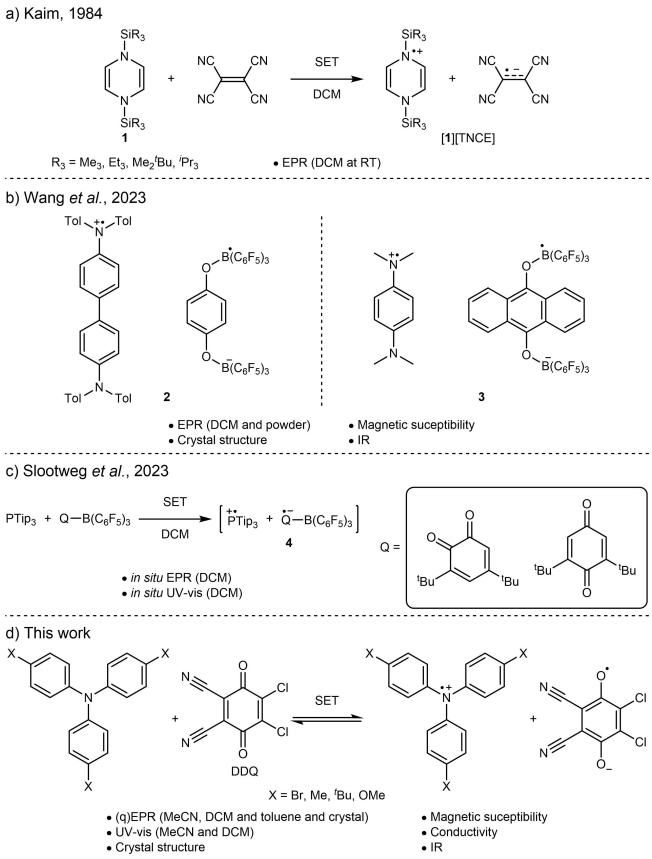

Scheme 1. Single-electron transfer (SET) in electron donor–acceptor systems forming radical ion pairs (RIPs)
a) The first direct evidence of thermal single-electron transfer involving main group reductants characterized in solution by EPR spectroscopy. b) Two stable, intermolecular RIPs using bis-amine based electron donors and Lewis acid activated quinone electron acceptors. c) Formation of quinone-based RIPs characterized in solution by UV–vis and EPR spectroscopy. d) The formation of stable RIPs using various triarylamines as the electron donor and DDQ as the electron acceptor.

electron donor.[12] Herein, we report the design of stable RIPs containing *para*-substituted triaryl amines as the electron donor, in combination with 2,3-dichloro-5,6-dicyano-1,4-benzoquinone (DDQ) as the electron acceptor (Scheme 1d), allowing full characterisation of the corresponding RIP $[(p\text{MeOPh})_3\text{N}]^{\bullet+}$ $[\text{DDQ}]^{\bullet-}$ in both solution and solid states. We also provide mechanistic rationale for the formation and degree of SET in RIPs.

Results and Discussion

First, we set out to determine the feasibility of thermal SET (ΔE_{SET}) for a series of *para*-substituted triarylamines ($(p\text{RPh})_3\text{N}$; R=Me_2N, MeO, PhO, Me, ^{t}Bu, Ph, F, Br, Cl, NO_2) to the electron-accepting DDQ using DFT calculations, with a dielectric solvent model representing acetonitrile and DCM, at the SCRF(MeCN/DCM)/(U)ωB97X–D/6-311 + G(d,p)//(U)ωB97X–D/6-31G(d) level of theory (Table S6). Gratifyingly, the selected arylamines cover the entire range from zero to complete charge transfer (e.g., ΔE_{SET} (MeCN) = +0.97 for R=NO_2, −0.91 eV for R=NMe_2; Figure 1). Their computed ionization energies (IEs; Figure 1) correlate well with the Hammett σ^+ values, similar to their electrochemically determined oxidation potentials, suggesting that the degree of charge transfer can be easily tuned.[13]

Next, we selected tris(*para*-bromophenyl)amine ($(p\text{BrPh})_3\text{N}$; IE_{MeCN} = +5.58 eV) as the electron donor, together with DDQ (EA_{MeCN} = −5.28 eV). DFT calculations indicate that the closed-shell encounter complex $[(p\text{BrPh})_3\text{N}, \text{DDQ}]$ is the ground state of this system (ΔE_{SET} (MeCN) = +0.30 eV), which was confirmed experimentally.[14] Furthermore, layering a yellow, equimolar solution of $(p\text{BrPh})_3\text{N}$ and DDQ in *ortho*-difluorobenzene with cyclohexane afforded bright green needles suitable for single-crystal X-ray diffraction (SC–XRD) analysis, confirming that no charge transfer had taken place. In the crystal (Figure 2),[15] the amine is combined with two equivalents of DDQ, all of which

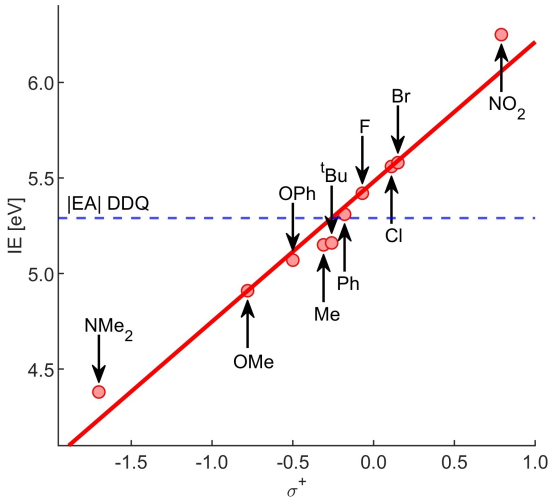

Figure 1. DFT calculated Hammett plot of the calculated ionization energies (IE) of *para*-substituted triaryl amines $(p\text{RPh})_3\text{N}$, together with the electron affinity of DDQ (blue dotted line) using an acetonitrile dielectric solvent model. Calculations were performed at the SCRF(MeCN)/(U)ωB97X–D/6-311 + G(d,p)//(U)ωB97X–D/6-31G(d) level of theory. Regression results: IE = 0.73 eV * σ^+ + 5.48 eV, R^2 = 0.959.

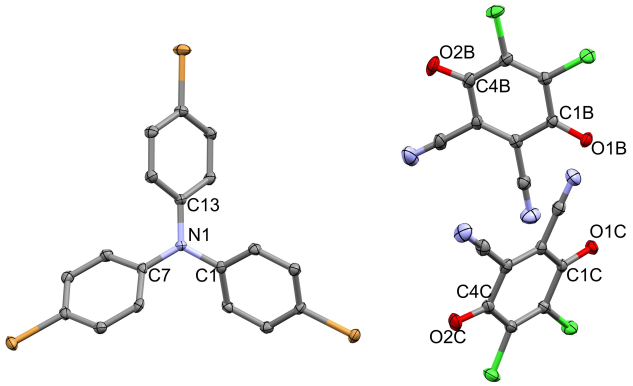

Figure 2. Molecular structure of $[(p\text{BrPh})_3\text{N}, \text{DDQ}]$. Hydrogen atoms were omitted for clarity. Displacement ellipsoids are drawn at a 50% probability level. Selected bond lengths [Å]: N1–C1 1.417(4), N1–C7 1.411(4), N1–C13 1.430(4), O1B–C1B 1.212(4), O2B–C4B 1.213(4), O1 C–C1 C 1.209(4), O2 C–C4 C 1.213(4).

show typical metrics of neutral molecules with an average C–N bond length of 1.419 Å (cf. 1.418 for (pBrPh)$_3$N vs. 1.411 Å for (pBrPh)$_3$N$^{\bullet+}$)[16] and an average C=O bond length of 1.213 and 1.211 Å (cf. an average of 1.217 for DDQ vs. 1.239 Å for [DDQ]$^{\bullet-}$; Table S3).[17] The closed-shell nature of [(pBrPh)$_3$N, DDQ] was also confirmed by its C=O IR stretching frequencies (1688 and 1674 cm^{-1}; Figure S31), which are similar to that of DDQ (1670 cm^{-1}), while its radical anion would lead to a shift to lower wavenumbers (cf. 1592–1552 cm^{-1} for [Fc][DDQ]).[18]

To promote charge transfer, we next focused on the more electron-donating tris(*para*-methylphenyl)amine (IE_{MeCN} = + 5.15 eV, ΔE_{SET} (MeCN) = −0.14 eV). Interestingly, treatment of (pMePh)$_3$N with DDQ in MeCN caused an instant colour change to purple, indicative of SET leading to the formation of the RIP [(pMePh)$_3$N]$^{\bullet+}$[DDQ]$^{\bullet-}$ (e.g., (pMePh)$_3$N$^{\bullet+}$, λ_{max} = 668 nm).[19] Yet, the reaction mixture was EPR silent, suggesting that the colour actually originates from a diamagnetic compound. Time-resolved *in situ* ^{1}H-NMR spectroscopy (Figure S13) showed the formation of two new doublets (AB-type; 3.67 and 3.54 ppm, $^2J_{H,H}$ = 14.1 Hz), revealing that C–H activation and functionalisation of one of the *para*-methyl groups occurred, affording a methylene moiety. Since prolonged reaction times did not result in full conversion to a single product, we assumed a non-selective reaction due to the presence of three equivalent methyl groups. To provide more insight, we employed the bulkier mono-*para*-methylphenylamine analogue (pMePh)(p^tBuPh)$_2$N (IE_{DCM} = + 5.25 eV, ΔE_{SET} (DCM) = + 0.08 eV) as the electron donor. Satisfyingly, after switching to DCM for solubility reasons and adding 1.0 equiv. of DDQ, the reaction mixture immediately yielded a persisted blue colour at ambient temperature (Scheme 2). After workup, dark blue crystals of **5** were obtained in 95% yield, also featuring two doublets (AB-type; 3.69 and 3.53 ppm, $^2J_{H,H}$ = 14.1 Hz) in the ^{1}H-NMR spectrum (Figure S2). The molecular structure of **5** in the crystal unequivocally established the formation of an adduct between two C–H activated tolylamines and one equiv. of DDQ, with the amines positioned in an *anti*-fashion at the cyano side of DDQ. Similar *anti*-adducts of DDQ have been isolated previously, but only in low yields using 1-methyl azulanes (3%)[20] or dipyrromethanes (25%).[21]

To detect the presumed radical ion pair intermediate [(pMePh)(p^tBuPh)$_2$N]$^{\bullet+}$[DDQ]$^{\bullet-}$, we employed *in situ* EPR spectroscopy. X-band EPR analysis at 100–150 K of a flash-frozen sample of the reaction mixture (taken immediately after mixing DCM solutions of (pMePh)(p^tBuPh)$_2$N and DDQ) confirmed the formation radical intermediates (Figure S16). The width of the signal (80 Gauss) and its shape at low temperatures resembles the signal we observed previously for [(pMePh)$_3$N]$^{\bullet+}$[B(C$_6$F$_5$)$_3$]$^{\bullet-}$, indicating the formation of an amine radical cation.[8a] Furthermore, for [(pMePh)$_3$N]$^{\bullet+}$[DDQ]$^{\bullet-}$, we were able to perform *in situ* EPR spectroscopy in MeCN at higher temperatures (up to 210 K; Figure S17) due to the higher melting point of MeCN compared to DCM. At 150 K, the spectra for [(pMePh)$_3$N]$^{\bullet+}$[DDQ]$^{\bullet-}$ and [(pMePh)(p^tBuPh)$_2$N]$^{\bullet+}$[DDQ]$^{\bullet-}$ have the same shape, while at 210 K a small signal (g_{iso} = ± 2.004) appears in the spectrum of [(pMePh)$_3$N]$^{\bullet+}$[DDQ]$^{\bullet-}$ that we attribute to [DDQ]$^{\bullet-}$. The low intensity of this signal suggests the formation of the [DDQ]$_2^{2-}$ dimer, as previously observed by us and Kochi et al.[9,22] Interestingly, the formation of **5** is much quicker in DCM than in benzene (± 6 h in CD_2Cl_2 vs ± 10 days in C_6D_6; Figures S10 and S11), as the polar RIP intermediate is better stabilised by the higher dielectric solvent, increasing its concentration (ΔE_{SET} = −0.08 (DCM) vs + 0.93 (benzene) eV). After the formation of [(pMePh)(p^tBuPh)$_2$N]$^{\bullet+}$[DDQ]$^{\bullet-}$, we postulate that the acidic tolylamine radical cation[23] is deprotonated by the [DDQ]$^{\bullet-}$ radical anion followed by subsequent radical coupling of the formed tolylamine and semiquinone radicals.[19] Another repetition of this sequence, affords **5** together with 2,3-dichloro-5,6-dicyanohydroquinone (**6**; Scheme 2), which we isolated in 38% yield.

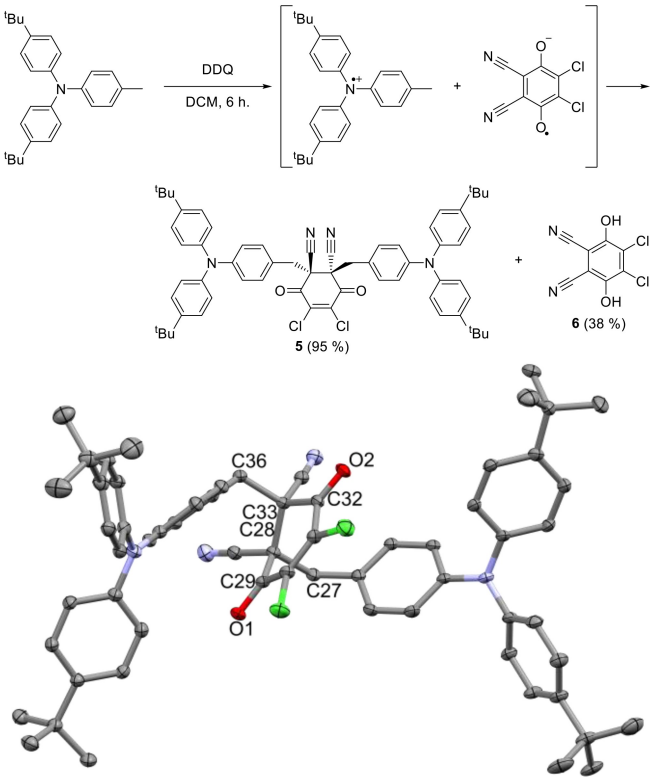

Scheme 2. Reaction of (pMePh)(p^tBuPh)$_2$N with DDQ affording **5** and **6** via the RIP [(pMePh)(p^tBuPh)$_2$]$^{\bullet+}$[DDQ]$^{\bullet-}$ intermediate (top) and the molecular structure of **5** (bottom). Hydrogen atoms were omitted for clarity. Displacement ellipsoids are drawn at a 50% probability level. Selected bond lengths [Å], angels and torsion angles [°] with the second independent molecule in square brackets: O1–C29 1.208 (3) [1.205 (4)], O2–C32 1.202 (3) [1.205 (3)], C28–C33 1.558 (4) [1.564 (4)], C27–C28–C33–C36 164.0 (2) [−175.2 (2)].

Avoiding reactive methyl groups entirely in the electron donor was achieved by using tris(4-*tert*-butylphenyl)amine (IE_{DCM} = + 5.26 eV; ΔE_{SET} (DCM) = + 0.08 eV), mixing with DDQ in DCM, as this amine is also poorly soluble in MeCN. Gratifyingly, an immediately and persistent green solution was obtained (Figure 3a). X-band EPR spectroscopy at ambient temperatures clearly feature signals attributable to both [(p^tBuPh)$_3$N]$^{\bullet+}$ (g_{iso} = 2.0031, a_{iso}(^{14}N) = 23.76 MHz)[24] and [DDQ]$^{\bullet-}$ (g_{iso} = 2.0054) in a near equimolar ratio, proving the formation of the RIP [(p^tBuPh)$_3$N]$^{\bullet+}$[DDQ]$^{\bullet-}$. UV–vis spectroscopy confirmed the presence of both [(p^tBuPh)$_3$N]$^{\bullet+}$ (λ_{max} = 681 nm)[22] and [DDQ]$^{\bullet-}$

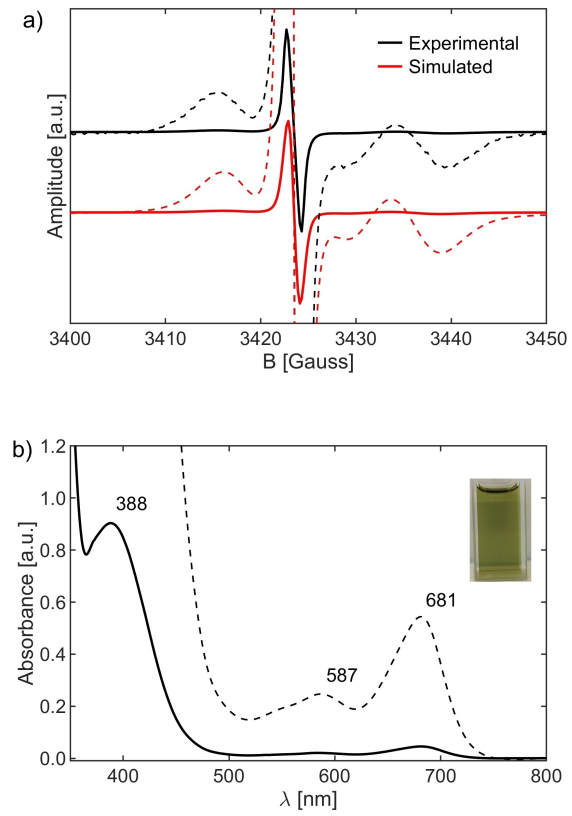

Figure 3. a) The room temperature X-band EPR spectrum of a DCM solution containing (p^tBuPh)$_3$N (20 mM) and DDQ (20 mM) with a simulation showing the presence of $[DDQ]^{\bullet-}$ ($g_{iso}=2.0054$) and $[(p^t BuPh)_3N]^{\bullet+}$ ($g_{iso}=2.0031$, $a_{iso}(^{14}N)=23.76$ MHz) in a 1:1.15 ratio. Dashed spectra shows zoom-in (25x). b) UV–vis spectrum of (p^tBuPh)$_3$N (1.0 mM) and DDQ (1.0 mM) in DCM. Dashed spectra represent the concentrated ((p^tBuPh)$_3$N (10 mM) and DDQ (10 mM)) and the photo thereof.

($\lambda_{max}=587$ nm; Figure 3b),[25] but the sizable absorption at $\lambda_{max}=388$ nm attributed to DDQ indicated only a modest conversion to the RIP.[26] We performed quantitative EPR (qEPR) measurements with TEMPO$^{\bullet}$, revealing a total radical concentration of about 0.2 mM from starting concentrations of 40 mM for both components. This result is consistent with observations from UV–vis suggesting only a small fraction of the amine and DDQ are converted to the RIP, confirming the endothermic nature of the formation as predicted by the calculated ΔE_{SET} (+0.08 eV in DCM).

To promote full charge transfer, we employed the more strongly donating tris(*para*-methoxyphenyl)amine ($IE_{MeCN}=+4.91$ eV; ΔE_{SET} (MeCN) $=-0.37$ eV), for which the resulting amine radical cation is even more stable than that of the previously used amines. Mixing equimolar amounts of (pMeOPh)$_3$N and DDQ in acetonitrile instantly afforded a blue solution indicative of SET and the formation of the $[(p\text{MeOPh})_3N]^{\bullet+}[DDQ]^{\bullet-}$ RIP. EPR spectroscopy confirmed the formation of $[(p\text{MeOPh})_3N]^{\bullet+}$ ($g_{iso}=2.0034$) with its characteristic ^{14}N-hyperfine coupling ($^{iso}a(^{14}N)=23.59$ MHz) and various hydrogen atoms ($^{iso}a(^{1}H)=5.18$ MHz (*m*-Ph*H*), 1.71 MHz (*o*-Ph*H*), 1.71 MHz (CH_3O); Figure 4a),[26] alongside the signal for $[DDQ]^{\bullet-}$ ($g_{iso}=2.0053$) with ^{14}N-hyperfine couplings to the nitrile groups ($a_{iso}(^{14}N)=1.60$ MHz).[27] UV–vis spectroscopy reinforced the formation of the $[(p\text{MeOPh})_3N]^{\bullet+}[DDQ]^{\bullet-}$ RIP, clearly demonstrating the presence of both $[(p\text{MeOPh})_3N]^{\bullet+}$ (718 nm)[16] and $[DDQ]^{\bullet-}$ (348, 456 and 600 nm; Figure 4b).[27]

The degree of charge transfer in equimolar solutions of (pMeOPh)$_3$N and DDQ was determined by employing a combination of qEPR and Evans NMR to measure the total radical concentration over a range of concentrations (Figure 4c). In MeCN, the total radical concentration is about half the starting concentration of the amine (or DDQ) over the investigated concentration range (1–25 mM). In DCM, at low concentrations ($\leq$15 mM of amine), the total radical concen-

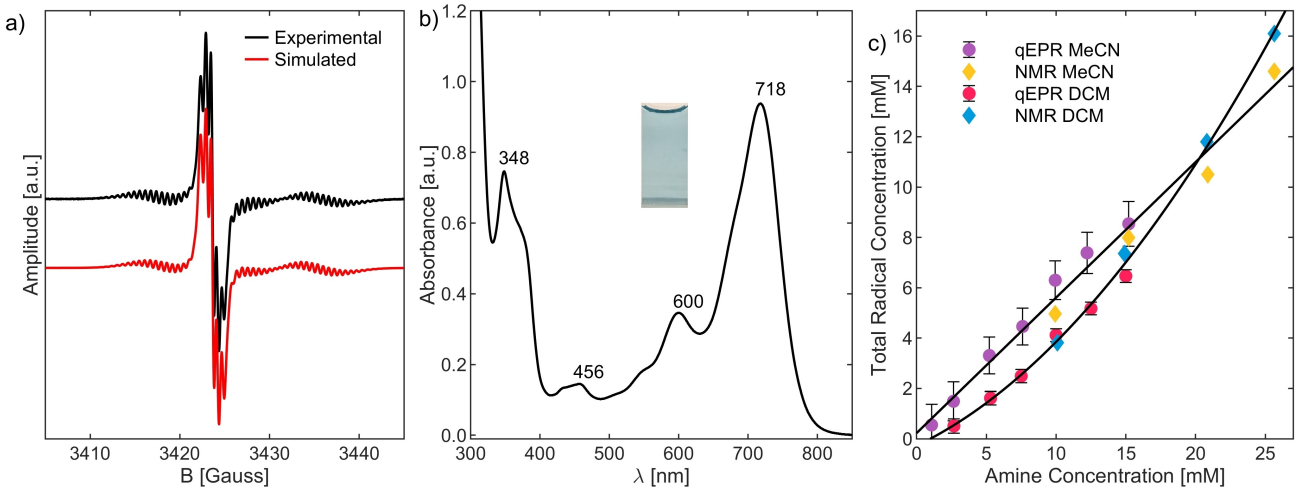

Figure 4. a) The room temperature X-band EPR spectrum of a MeCN solution containing (pMeOPh)$_3$N (1.0 mM) and DDQ (1.0 mM) with a simulation showing the presence of both $[DDQ]^{\bullet-}$ ($g_{iso}=2.0053$, 2x $a_{iso}(^{14}N)=1.60$ MHz) and $[(p\text{MeOPh})_3N]^{\bullet+}$ ($g_{iso}=2.0034$, $a_{iso}(^{14}N)=23.59$ MHz, 6x $a_{iso}(^{1}H)=5.18$ MHz (*m*-Ph*H*), 6x 1.71 MHz (*o*-Ph*H*), 9x 1.71 MHz (CH_3O)) in a 1:0.96 ratio. b) UV–vis spectrum of (pMeOPh)$_3$N (0.1 mM) and DDQ (0.1 mM) in MeCN with a photograph of the sample inset. c) Determination of the total radical concentration of solutions of $[(p\text{MeOPh})_3N]^{\bullet+}[DDQ]^{\bullet-}$ in both MeCN and DCM using qEPR and Evans NMR. Error bars are drawn to show the 90% confidence intervals of the qEPR measurements. Regression results for MeCN: $y=0.538 * x+0.227$, $R^2=0.982$; for DCM: $y=0.0147 * x^2+0.266 * x-0.27$, $R^2=0.998$.

tration is lower than equivalent MeCN solutions, as expected based on the solvent's lower polarity and, therefore, reduced ability to stabilize the charges of the RIP. This is also reflected in the calculated ΔE_{SET} (−0.17 eV in DCM vs. −0.37 eV in MeCN). Conversely, more concentrated solutions reveal higher radical concentrations in DCM rather than in MeCN (15.5 mM vs. 13.9 mM, respectively, using 25 mM amine and DDQ). We ascribe this non-linearity to the double reduction of DDQ to the dianion, as electrochemical studies have shown that the second reduction of DDQ is more facile in DCM than in MeCN.[28] Lastly, we utilized toluene as solvent (ΔE_{SET} (toluene) = +0.62 eV), which resulted in only about 7 μM of radicals when using 40 mM of (*p*MeOPh)$_3$N and DDQ, reinforcing our observation that solvent polarity plays a major role in the total degree of SET achieved in solution.

Violet single crystals of [(*p*MeOPh)$_3$N]$^{\bullet+}$[DDQ]$^{\bullet-}$ suitable for SC–XRD analysis were obtained by storing a dark blue, equimolar solution of (*p*MeOPh)$_3$N and DDQ in CD_3CN at −30 °C, which showed that in one unit cell one (*p*MeOPh)$_3$N and two molecules of DDQ are stacked, of which one DDQ is shared with the neighbouring unit cell (Figure 5).[13] The electron donor shows typical metrics for oxidised (*p*MeOPh)$_3$N with an average shortened C–N and C–O bond lengths of 1.409 and 1.352 Å, respectively (cf. 1.409 and 1.378 for (*p*MeO*m*^{t}Bu$_2$Ph)$_3$N$^{\bullet+}$ vs. 1.426 and 1.392 Å for (*p*MeO*m*^{t}Bu$_2$Ph)$_3$N, respectively).[29] Analysis of the C–O bonds of the two DDQ acceptor molecules showed that DDQ–C, located further from the donor component, is significantly more reduced than DDQ–B, as the average C–O bond is longer (1.233 Å for DDQ–C and 1.223 Å for DDQ–B) and closer to the reported bond length of [DDQ]$^{\bullet-}$ (cf. an average of 1.239 Å for [DDQ]$^{\bullet-}$ vs 1.217 for DDQ; Table S3).[16] The weakening of the DDQ C=O bond upon reduction was also confirmed by its reduced IR stretching frequencies (1574 and 1564 cm^{-1}, Figure S31; cf. 1592–1552 cm^{-1} for [Fc][DDQ] vs. 1670 cm^{-1} for DDQ).[17]

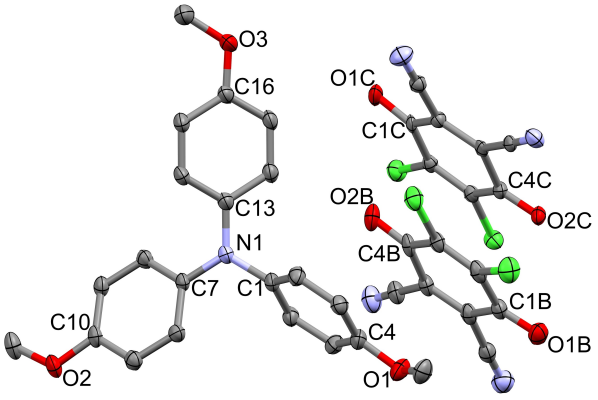

Figure 5. Molecular structure of (*p*MeOPh)$_3$N{DDQ}$_{1.5}${CD$_3$CN}$_2$ in the crystal. Hydrogen atoms and co-crystallized CD_3CN were omitted for clarity. Displacement ellipsoids are drawn at a 50% probability level. Selected bond lengths [Å]: N1–C1 1.428(5), N1–C7 1.407(5), N1–C13 1.392(6),O1–C4 1.359(5), O2–C10 1.350(5), O3–C16 1.348(5), O1B–C1B 1.217(6), O2B–C4B 1.230(6), O1 C–C1 C 1.231(10), O2 C–C4 C 1.235(12).

To further characterise the paramagnetic character of [(*p*MeOPh)$_3$N]$^{\bullet+}$[DDQ]$^{\bullet-}$, we recorded the X-band EPR spectrum of a single crystal at 298 K, which revealed a relatively narrow signal (FWHM = ±3.4G) attributed to [DDQ]$^{\bullet-}$ (Figure 6a). For [(*p*MeOPh)$_3$N]$^{\bullet+}$, a significant ^{14}N-hyperfine is expected; however, this signal is presumably absent due to strong antiferromagnetic coupling between two neighbouring amines via π-π-stacking of the aryl groups (3.50 Å between the aryl groups as shown in the crystal structure).[30] Interestingly, the intensity of the EPR signal of this crystal is temperature-dependent, increasing as the temperature rises (Figure 6b). This suggests an open-shell (EPR-silent) singlet ground state with a thermally excited (EPR-active) triplet state.[4] Indeed, fitting the Bleaney–Bowers equation[31] yielded an electronic coupling of $-2J = 241 \pm 63$ cm^{-1} (0.69 ± 0.18 kcal mol^{-1}), confirming that the triplet state is thermally accessible.

DFT calculations on the molecular structure of [(*p*MeOPh)$_3$N]$^{\bullet+}$[(DDQ)$_2$]$^{\bullet-}$ in the crystal show that combining the electron donor and acceptor molecules initially forms the closed-shell EDA complex [(*p*MeOPh)$_3$N][(DDQ)$_2$]. Subsequent SET leads to the thermodynamically favoured open-shell singlet RIP ^{1}[(*p*MeOPh)$_3$N]$^{\bullet+}$[(DDQ)$_2$]$^{\bullet-}$ ($\Delta E = -5.4$ kcal mol^{-1}; Fig-

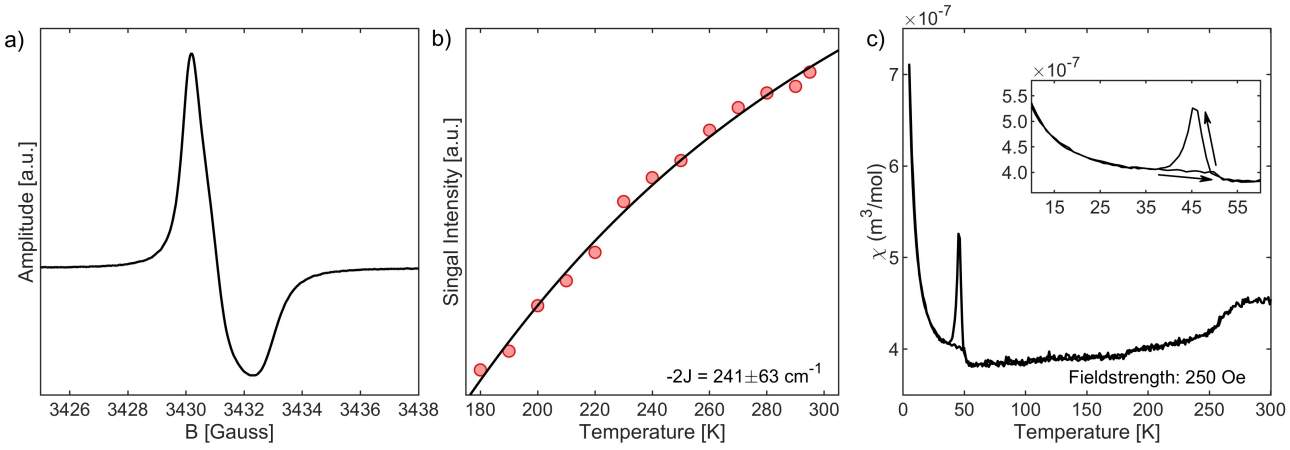

Figure 6. a) The X-band room temperature EPR spectrum of a single crystal of {(*p*MeOPh)$_3$N}$_2${DDQ}$_3${CD$_3$CN}$_4$. b) Temperature dependence of the EPR signal intensity and fit with the Bleaney–Bowers equation. c) Magnetic susceptibility of {(*p*MeOPh)$_3$N}$_2${DDQ}$_3${CD$_3$CN}$_4$ measured by SQUID with a magnetic field of 25 mT.

ure S36). Intersystem crossing (ISC) can then afford the EPR-active triplet RIP $^3[(p\text{MeOPh})_3\text{N}]^{\bullet+}[(\text{DDQ})_2]^{\bullet-}$, which is slightly endothermic ($\Delta E = +0.42$ kcal mol^{-1}) but thermally accessible, as observed experimentally by EPR spectroscopy. Analysis of the charge distribution revealed that $(p\text{MeOPh})_3\text{N}$ is almost fully oxidized (Hirshfeld charge $= +0.70$ for the open-shell singlet state and $+0.72$ for the triplet state). Consistent with the SC–XRD structure analysis, only one of the two DDQ molecules is almost fully reduced (-0.62 and -0.08 for the open-shell singlet state vs. -0.60 and -0.10 for the triplet state). Additionally, SQUID magnetic measurements of crystalline $[(p\text{MeOPh})_3\text{N}]^{\bullet+}[(\text{DDQ})_{1.5}]^{\bullet-}$ in a magnetic field of 25 mT (Figure 6c) show that χ values gradually increase from $3.8{\cdot}10^{-7}$ to $4.5{\cdot}10^{-7}$ m^3 mol^{-1} from 60 to 300 K, respectively, underlining the presence of an accessible thermally excited triplet state. Note, the peak at 45 K is likely caused by absorbed oxygen during sample preparation, while below 35 K, the susceptibility is dominated by a paramagnetic impurity, as previously reported for [pyridinium]$^{\bullet+}$[DDQ]$^{\bullet-}$ salts.[32] As expected, the magnetic susceptibility of the crystalline closed-shell, diamagnetic encounter complex $[(p\text{BrPh})_3\text{N}, (\text{DDQ})_2]$ showed the opposite trend, with slightly decreasing χ values from $0.29{\cdot}10^{-7}$ to $0.26{\cdot}10^{-7}$ m^3 mol^{-1} from 60 to 300 K (in a magnetic field of 100 mT; Figure S33). For this neutral complex, DFT calculations confirm the ground state to be a closed-shell singlet with minimal charge transfer ($+0.12$ for $(p\text{BrPh})_3\text{N}$ and -0.07 and -0.05 for DDQ–B and DDQ–C, respectively) and an inaccessible triplet state ($\Delta E_{\text{CS–T}} = 13.1$ kcal mol^{-1}).[33]

Conclusions

We successfully demonstrated the design of persistent intermolecular radical ion pairs based on amines and the strongly oxidising DDQ as an electron acceptor. By determining the ionization energies (IE) of *para*-substituted arylamines and the electron affinity (EA) of DDQ, we were able to predict the occurrence of single-electron transfer (SET). When using $(p\text{BrPh})_3\text{N}$, no charge transfer was observed in either solution or solid states. In contrast, combining $(p\text{MePh})_3\text{N}$ with DDQ resulted in C–H activation of the methyl group, which was ultimately confirmed using $(p\text{MePh})(p^t\text{BuPh})_2\text{N}$. The stability of the *tert*-butyl groups allowed $(p^t\text{BuPh})_3\text{N}$ to serve as the electron donor, leading to the formation of the first stable triarylamine–quinone radical ion pair in solution. Characterization using both UV–vis and (q)EPR spectroscopy confirmed the presence of both the radical cation and anion, although conversion to the RIP was low. Switching to the more electron-donating $(p\text{MeOPh})_3\text{N}$ resulted in a higher degree of conversion to the open-shell RIP $^1[(p\text{MeOPh})_3\text{N}]^{\bullet+}[\text{DDQ}]^{\bullet-}$ due to a more stabilized amine radical cation. The degree of charge transfer was significantly influenced by solvent polarity, as more polar solvents better stabilize the charges of the RIP. Furthermore, in the crystal phase, we demonstrated the presence of charge transfer and the formation of a thermally accessible, EPR-active triplet state. Overall, we demonstrate the ability to control the degree of SET within donor–acceptor systems in both solution and solid state, and we showcased that fleeting frustrated radical pairs can be readily tuned to allow the isolation and full characterisation of stable, isolable species. We are currently expanding the scope of electron donors and acceptors to further tune the RIPs for reactivity with external substrates.

Acknowledgements

This work was financially supported by the Netherlands Organization for Scientific Research (NWO) in the framework of the Science PPP Fund for the top sectors via an ENW PPS LIFT grant (ENPPS.LIFT.019.009) and Shell Global Solutions International BV.

Conflict of Interests

The authors declare no conflict of interest.

Data Availability Statement

The data that supports the findings of this study are available in the supplementary material of this article. The supporting information contains synthetic procedures, spectroscopic and computational methods, and (additional) spectra.

Keywords: Radical ion pairs · Frustrated radical pairs · Frustrated Lewis pairs · Single-electron transfer · Organic radicals

[1] M. Yan, J. C. Lo, J. T. Edwards, P. S. Baran, *J. Am. Chem. Soc.* **2016**, *138*(39), 12692–12714.
[2] W. Kaim, *Angew. Chem. Int. Ed. Engl.* **1984**, *23*(8), 613–614; *Angew. Chem.* **1984**, *96*(8), 609–610.
[3] For a recent review on organic donor-acceptor complexes see: a) C. Mathur, R. Gupta, R. K. Bansal, *Chem. - Eur. J.* **2024**, *30*, e202304139; For examples of the use of DDQ as electron acceptor in these complexes, see: b) S. Mohamud, V. T. Phuoc, L. del Campo, N. E. Massa, S. Pagola, *Synth. Met.* **2016**, *214*, 71–75; c) M. S. Fonari, S. Rigin, D. Lesse, T. V. Timofeeva, *J. Mol. Struct.* **2023**, *1278*, 134900.
[4] S. Kong, S. Tang, T. Wang, Y. Zhao, Q. Sun, Y. Zhao, X. Wang, *CCS Chem.* **2023**, *5*, 334–340.
[5] For intermolecular variants, see: a) J. Wang, H. Cui, H. Ruan, Y. Zhao, L. Zhang, X. Wang, *J. Am. Chem. Soc.* **2022**, *144*, 7978–7982; b) S. Kong, L. Yang, Q. Sun, T. Wang, R. Pei, Y. Zhao, W. Wang, Y. Zhao, H. Cui, X. Gu, X. Wang, *Angew. Chem. Int. Ed.* **2024**, *63*, e202400913; *Angew. Chem.* **2024**, *136*, e202400913.
[6] For an all-boron based RIP generated from a strongly reducing diborene donor and a borole acceptor, see: H. Bissingersee: P. Braunschweig, A. Damme, C. Hörl, I. Krummenacher, T. Kupfer, *Angew. Chem. Int. Ed.* **2015**, *54*(1), 359–362; *Angew. Chem.* **2015**, *127*, 366–369.
[7] a) L. L. Liu, D. W. Stephan, *Chem. Soc. Rev.* **2019**, *48*, 3454–3463; b) A. Dasgupta, E. Richards, R. L. Melen, *Angew. Chem. Int. Ed.* **2021**, *60*, 53–65; *Angew. Chem.* **2021**, *133*, 53–65; c) L. L. Liu, L. L. Cao, Y. Shao, G. Ménard, D. W. Stephan, *Chem.* **2017**, *3*, 259–267; d) L. L. Liu, L. L. Cao, D. Zhu, J. Zhou, D. W. Stephan, *Chem. Commun.* **2018**, *54*, 7431–7434; e) A. Merk, H. Großekappenberg, M. Schmidtmann, M.-P. Luecke, C. Lorent, M. Driess, M. Oestreich, H. F. T. Klare, T. Müller, *Angew. Chem. Int. Ed.* **2018**, *57*, 15267–15271; *Angew. Chem.* **2018**, *130*, 15487–15492; f) Y. Soltani, A. Dasgupta, T. A. Grazis, D. M. C. Ould, E. Richards, B. Slater, K. Stefkova, V. Y. Vladimirov, L. C. Wilkins, D. Wilcox, R. L. Melen, *Cell Rep. Phys. Chem.* **2020**, *1*, 100016; g) Y. Aramaki, N. Imaizumi, M. Hotta, J.

Kumagi, T. Ooi, *Chem. Sci.* **2020**, *11*, 4305–4311; h) A. Dasgupta, K. Stefkova, R. Babaahmadi, B. F. Yates, N. J. Buurma, A. Ariafard, E. Richards, R. L. Melen, *J. Am. Chem. Soc.* **2021**, *143*, 4451–4464.
[8] For recent reviews on radicals in main-group chemistry, see: a) L. J. C. van der Zee, S. Pahar, E. Richards, R. L. Melen, J. C. Slootweg, *Chem. Rev.* **2023**, *123*, 9653–9675; b) L. J. C. van der Zee, J. Hofman, J. M. van Gaalen, J. C. Slootweg, *Chem. Soc. Rev.* **2024**, *53*, 4862–4876.
[9] a) F. Holtrop, A. R. Jupp, N. P. van Leest, M. Paradiz Dominguez, R. M. Williams, A. M. Brouwer, B. de Bruin, A. W. Ehlers, J. C. Slootweg, *Chem. - Eur. J.* **2020**, *26*(41), 9005–9011; b) F. Holtrop, A. R. Jupp, B. J. Kooij, N. P. van Leest, B. de Bruin, J. C. Slootweg, *Angew. Chem. Int. Ed.* **2020**, *59*, 22210–22216; *Angew. Chem.* **2020**, *132*, 22394–22400.
[10] C. Helling, L. J. C. van der Zee, J. Hofman, F. J. de Zwart, S. Mathew, M. Nieger, J. C. Slootweg, *Angew. Chem. Int. Ed.* **2023**, *62*, e202313397; *Angew. Chem.* **2023**, *135*, e202313397.
[11] M. Ju, Z. Lu, L. F. T. Novaes, J. I. Martinez Alvarado, S. Lin, *J. Am, Chem. Soc.* **2023**, *145*, 19478–19489.
[12] S. Wu, J. Žurauskas, M. Domański, P. S. Hitzfeld, V. Butera, D. J. Scott, J. Rehbein, A. Kumar, E. Thyrhaug, J. Hauer, J. P. Barham, *Org. Chem. Front.* **2021**, *8*, 1132–1142.
[13] S. Dapperheld, E. Steckhan, K.-H. Grosse Brinkhaus, T. Esch, *Chem. Ber.* **1991**, *124*, 2557–2567.
[14] Treatment of $(p\text{BrPh})_3\text{N}$ with DDQ in acetonitrile afforded a yellow solution that featured a sharp signal in the EPR spectrum (Figure S1), which we attributed to a background signal of $[\text{DDQ}]^{\bullet-}$.
[15] CCDC deposition number(s) https://www.ccdc.cam.ac.uk/services/structures?id=doi:10.1002/chem.20240388523752 39 ($\{(p\text{BrPh})_3\text{N}\}\{\text{DDQ}\}_2$), 2375241 ($(^t\text{BuPh})_2(\text{CH}_3\text{Ph})\text{N}-\text{DDQ}$ adduct), and 2375240 ($\{(p\text{MeOPh})_3\text{N}\}_2\{\text{DDQ}\}_3\{\text{CD}_3\text{CN}\}_4$) contain the supplementary crystallographic data for this paper. These data are provided free of charge by the joint Cambridge Crystallographic Data Centre and Fachinformationszentrum Karlsruhe Access Structures service https://www.ccdc.cam.ac.uk/structures.
[16] M. Quiroz-Guzman, S. N. Brown, *Acta Cryst.* **2010**, *C66*, m171–m173.
[17] V. Rasokha, J. Lu, T. Y. Rosokha, J. K. Kochi, *Phys. Chem. Chem. Phys.* **2009**, *11*, 324–332.
[18] H. M. A. Salman, M. R. Mahmoud, M. H. M. Abou-El-Wafa, U. M. Rabie, R. H. Crabree, *Inorg. Chem. Comm.* **2004**, *7*(11), 1209–1212.
[19] B. N. DiMarco, L. Troian-Gautier, R. N. Sampaio, G. J. Meyer, *Chem. Sci.* **2018**, *9*, 940–949.
[20] a) R. Sigrist, H.-J. Hansen, *Helv. Chim. Acta* **2010**, *93*(8), 1545–1567; b) R. Sigrist, H.-J. Hansen, *Helv. Chem. Acta* **2010**, *93*(8), 1568–1582.
[21] a) J.-Y. Shin, B. O. Patrick, D. Dolphin, *Org. Biomol. Chem.* **2009**, *7*, 2032–2035; b) J.-Y. Shin, D. Dophin, *New J. Chem.* **2011**, *35*, 2483–2487.
[22] a) J.-M. Lü, S. V. Rosokha, J. K. Kochi, *J. Am. Chem. Soc.* **2003**, *125*, 12161–12171; b) V. Ganesan, S. V. Rosokha, J. K. Kochi, *J. Am. Chem. Soc.* **2003**, *125*, 2559–2571; c) J. S. Miller, P. J. Krusic, D. A. Dixon, W. M. Reiff, J. H. Zhang, E. C. Anderson, A. J. Epstein, *J. Am. Chem. Soc.* **1986**, *108*, 4459–4466.
[23] M. Schmittel, A. Burghart, *Angew. Chem. Int. Ed. Engl.* **1997**, *36*, 2550–2589; *Angew. Chem.* **1997**, *109*, 2658–2699.
[24] T. Michinobu, E. Tsuchida, H. Nishide, *Bull. Chem. Soc. Jpn.* **2000**, *73*, 1021–1027.
[25] a) J. S. Miller, P. J. Krusic, D. A. Dixon, W. M. Reiff, J. H. Zhang, E. C. Anderson, A. J. Epstein, *J. Am. Chem. Soc.* **1986**, *108*, 4459–4466; b) J.-M. Lü, S. V. Rosokha, J. K. Kochi, *J. Am. Chem. Soc.* **2003**, *125*, 12161–12171; c) V. Ganesan, S. V. Rosokha, J. K. Kochi, *J. Am. Chem. Soc.* **2003**, *125*, 2559–2571; d) S. V. Rosokha, J. Lu, T. Y. Rosokha, J. K. Kochi, *Phys. Chem. Chem. Phys.* **2009**, *11*, 324–332.
[26] S. Mallick, S. Maddala, K. Kollimanlayan, P. Venkatakrishnan, *J. Org. Chem.* **2019**, *84*(1), 73–93.
[27] D. Gordon, M. J. Hove, *J. Chem, Phys.* **1973**, *59*, 3419–3420.
[28] R. Patricia-Andrea Staley, E. M. Lopez, L. A. Clare, D. K. Smith, *J. Phys. Chem. C.* **2015**, *119*(35), 20319–20327.
[29] M. Zhou, L. Mao, *Chin. Chem. Lett.* **2022**, *33*(4), 1870–1874.
[30] Antiferromagnetic coupling between two radicals in close approximaty was also observed by Stoddart et al. in dimeric tetrahiafulvalane [3]catenanes: a) J. M. Spruell, A. Coskun, D. C. Friedman, R. S. Forgan, A. A. Sarjeant, A. Trabolsi, A. C. Fahrenbach, G. Barin, W. F. Paxton, S. K. Dey, M. A. Olson, D. Benítez, E. Tkatchouk, M. T. Colvin, R. Carmielli, S. T. Caldwell, G. M. Rosair, S. Gunatilaka Hewage, F. Duclairoir, J. L. Seymour, A. M. Z. Slawin, W. A. Goddard III, M. R. Wasielewski, G. Cooke, J. F. Stoddart, *Nat. Chem.* **2010**, *2*, 870–879; b) A. Coskun, J. M. Spruell, G. Barin, A. C. Fahrenbach, R. S. Forgan, M. T. Colvin, R. Carmieli, D. Benítez, E. Tkatchouk, D. C. Friedman, A. A. Sarjeant, M. R. Wasielewski, W. A. Goddard III, J. F. Stoddart, *J. Am. Chem. Soc.* **2011**, *133*(12), 4538–4547.
[31] In the Bleaney-Bowers equation, the $1/(3+\exp(-2\ \text{J/T*Kb}))$ term relates the magnetic susceptibility due to the thermal occupation of a triplet state. As the intensitiy of the EPR signal also depends on the occupation of the triplet state, the $1/(3+\exp(-2\ \text{J/T*Kb}))$ term also relates the EPR signal intensity to the occupation of the triplet state, see: a) B. Bleaney, K. D. Bowers, *Proc. R. Soc. London, Ser. A* **1952**, *214*, 451–465; b) R. Calvo, R. P. Sartoris, A. R. Nascimento, M. Šedivý, A. Sojka, P. Neugebauer, V. T. Santana, *Coord. Chem. Rev.* **2023**, *480*, 215007.
[32] P. Stanić, D. Barašić, D. Pajić, A. Štantić, K. Molčanov, *Cryst. Growth. Des.* **2022**, *22*, 6461–6471.
[33] We investigated the conductivity of both crystals and found them to be insulators, potentially due to the absorption of oxygen at the crystal, unlike dibenzotetrathiafulvalene−DDQ CT-complexes that showed to be conductors ($8\ \Omega^{-1}\text{cm}^{-1}$), see: J. J. Mayerle, J. B. Torrance, *Bull. Chem. Soc. Jpn.* **1981**, *54*(10), 3170–31720.

Manuscript received: November 6, 2024
Accepted manuscript online: November 8, 2024
Version of record online: November 22, 2024